Longwave Broken Cloud Approximations Allowing for Cloud Transmission

E. E. Takara and R. G. Ellingson
University of Maryland
College Park, Maryland

Abstract

Cloud transmission, absorption, emission, and scattering in the 8-μm to 12-μm window region is an important factor in the earth's radiative energy budget. Recent work in the window region (Takara and Ellingson 1999) has shown that clouds can be modeled as black with very little error except when the clouds are optically thin. It concluded that scattering was not important. In this work, clouds are approximated as transmitting, absorbing, and emitting bodies; scattering is neglected. The approximation works well for surface fluxes, but not as well for upward fluxes above the clouds.

Introduction

Absorption by atmospheric gases dominates radiative transfer in the longwave spectrum. The major exception to this is the atmospheric window (8 μm to 12 μm), where gaseous absorption is relatively low. In clear-sky conditions, heat emitted from the surface in the window region is transmitted with very little attenuation to the top of the atmosphere. Clouds can have a major effect on climate by affecting the radiative transfer in the window region.

Modeling the one-dimensional radiative transfer through a homogenous, plane-parallel cloud becomes more complicated when the cloud scatters. When the cloud is broken up into a field of cloud elements surrounded by clear air, computing the radiative transfer becomes a complex three-dimensional problem. To simplify this problem, general circulation models (GCMs) compute the upward or downward fluxes from broken cloud fields $F^{\uparrow\downarrow}$, by averaging clear-sky and overcast-sky fluxes:

$$F^{\uparrow\downarrow} = N\, F^{\uparrow\downarrow}(\text{overcast}) + (1-N)\, F^{\uparrow\downarrow}(\text{clear}) \qquad (1)$$

$F^{\uparrow\downarrow}$ (overcast) and $F^{\uparrow\downarrow}$ (clear) are the plane-parallel solutions for completely overcast and completely clear skies.

In Takara and Ellingson (1999), it was shown that modeling water clouds as black bodies (the black cloud approximation) worked well if the clouds were optically thick. It failed for optically thinner water clouds because they allowed a significant amount of transmission. Longwave scattering by water clouds was not as important as transmission through optically thin clouds. If longwave scattering can be neglected, it would greatly simply the radiative transfer problem. Narrowband transmission models ignore scattering, such as the Maryland Terrestrial Radiation Package (MDTERP) (Ellingson and Takara

1999), could be used directly. In this work, the accuracy of modeling water clouds as transmitting, absorbing, and emitting bodies (the no-scatter approximation) is examined.

Computation

The window region fluxes are found by spectral and angular integration of radiances. The spectral integration is performed by discretizing the window region into six intervals. The "monochromatic" upward and downward radiances, $I^{\uparrow\downarrow}$, were computed by summing over the wavelength (λ) intervals.

$$I^{\uparrow\downarrow} = \int_{8\mu m}^{12\mu m} I_{\lambda}^{\uparrow\downarrow} d\lambda = \sum_{i=1}^{6} I_{i}^{\uparrow\downarrow} \Delta\lambda \tag{2}$$

$I_i^{\uparrow\downarrow}$ is the spectral radiance or specific intensity of the ith wavelength interval. The intervals are: 8 μm $\leq \lambda_1 \leq$ 8.25 μm $\leq \lambda_2 \leq$ 8.75 μm $\leq \lambda_3 \leq$ 9.25 μm $\leq \lambda_4 \leq$ 10 μm $\leq \lambda_5 \leq$ 11 μm $\leq \lambda_6 \leq$ 12 μm.

The upward and downward flux is found by Gaussian quadrature for three angles.

$$F^{\uparrow\downarrow} = \int_0^{\pi/2} I^{\uparrow\downarrow}(\theta)\cos(\theta)d\theta = \sum_{j=1}^{3} w_{gj} I_i^{\uparrow\downarrow} \tag{3}$$

The radiative transfer within the layer was modeled using the Monte Carlo method (Howell and Perlmutter 1964). A more detailed description of the computational method can be found in Takara and Ellingson (1999).

Assumptions and Parameters

The cloud field is a single layer of identical randomly overlapping cylinders with a uniform cloud base altitude as in Ellingson (1982), Figure 1. The clouds are homogenous with the same temperature profile as the surrounding air; the temperature variation between levels is assumed to be linear. Lastly, the surface is black. The McClatchey soundings (McClatchey et al. 1971) were used for temperature and species profiles. Results for the mid-latitude summer (MLS) and mid-latitude winter (MLW) soundings are presented here.

The fluxes are computed for two pairs of cloud aspect ratios (α) and diameter (D): the small flat cloud set, α=0.5 km; D=0.25 km, cloud thickness of 0.125 km and the larger set α=1 km and D=1 km, cloud thickness of 1 km. The base cloud fraction (N) and cloud base altitude (Z_b) is also varied. N values are 0.1, 0.3, 0.5, 0.7, 0.9, and 1. Z_b values are 0.5 km, 2 km, and 4 km for water clouds.

The water cloud equivalent radius (R_{eq}) (Hu and Stamnes 1993) was set at 3 μm, 5 μm, and 10 μm. The liquid water content (LWC) is 0.1 g*m^{-3} for MLW and 0.2g*m^{-3} for MLS.

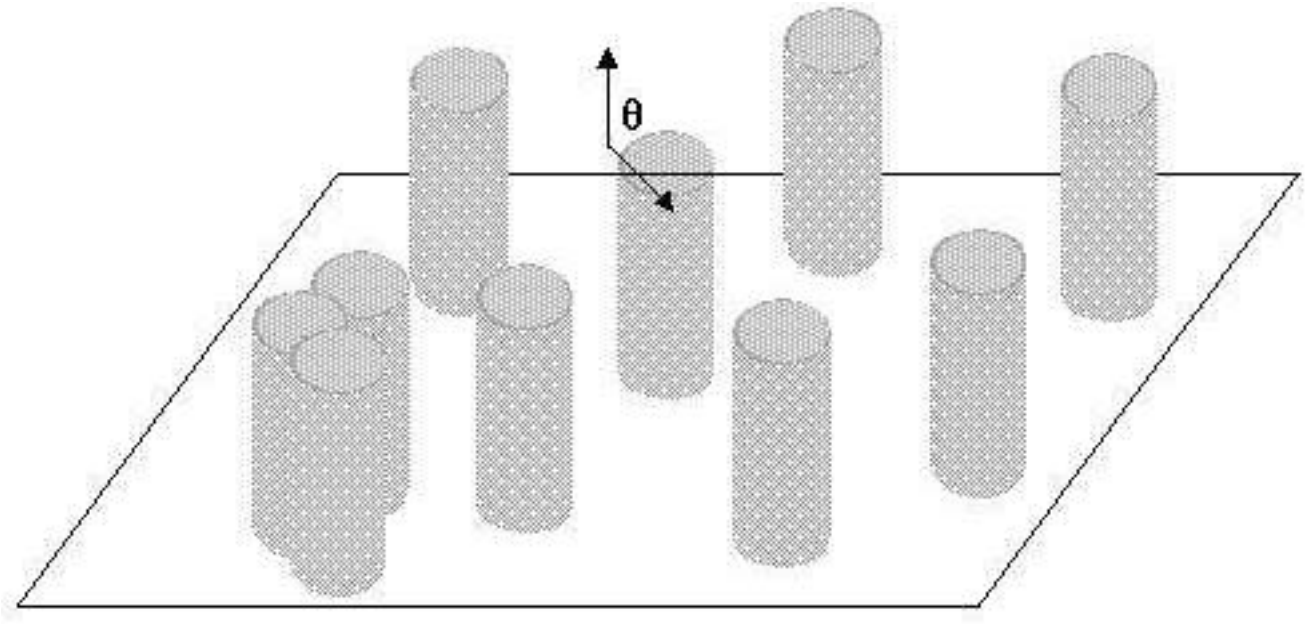

Figure 1. A single layer of cylindrical clouds allowed to merge.

The cloud extinction coefficient (β_{ext}), single-scattering albedo (ω), and asymmetry factor (g) from the parameterizations of Hu and Stamnes (1993) for water clouds are averaged over each wavelength interval. They are shown in Figures 2a, 2b, and 2c.

Results

The downward flux at the surface as a function of base cloud fraction (N) for the MLS and MLW atmospheres is shown in Figures 3a and 3b. Solid lines are used for the large clouds (α=1 D=1 km), dashed lines for the small clouds (α=0.5 D=0.25 km). The symbols are centered on the fluxes for R_{eq}=5 μm; limit bars show results for the other R_{eq}=3 μm and 5 μm. This line and symbol convention is used in all subsequent figures.

Figures 3a and 3b have some similarities. They rise from minima for clear skies (N=0) to maxima for completely overcast skies (N=1). The fluxes decrease as Z_b increases. For a given Z_b, the large cloud flux is larger than the small cloud flux. In Figure 3a, the small cloud flux is almost the same as the large cloud flux for N=1; the N=1 fluxes are noticeably different in Figure 3b. This can be attributed to the clouds' larger optical thickness in Figure 3a; the fluxes are almost the same in Figure 3a because both the small and large clouds are opaque when N=1. In Figures 3a and 3b, the large cloud limit bars are both very small. But the limit bars in Figure 3b are noticeably larger than the limit bars in Figure 3a. The changes in ω and g (which depend on R_{eq}) are more apparent when the clouds are optically thinner.

The upward fluxes at 15 km for MLS and MLW are shown in Figures 4a and 4b. The maxima are for clear skies and the maxima are for completely cloudy skies. The fluxes decrease as Z_b increases. For a

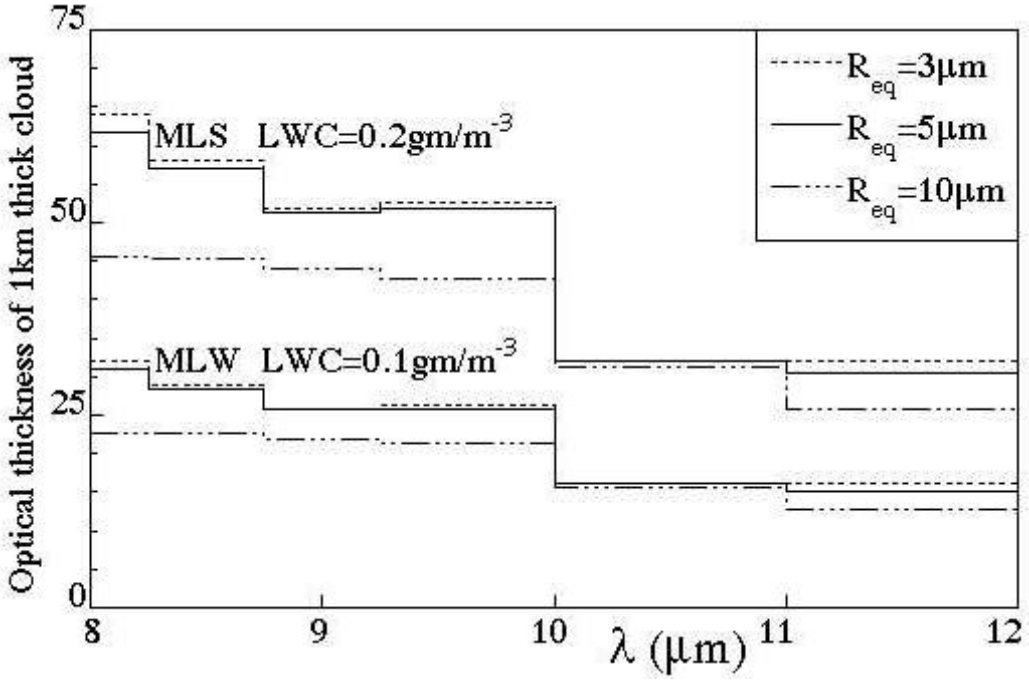

Figure 2a. Optical thickness of 1-km thick water clouds.

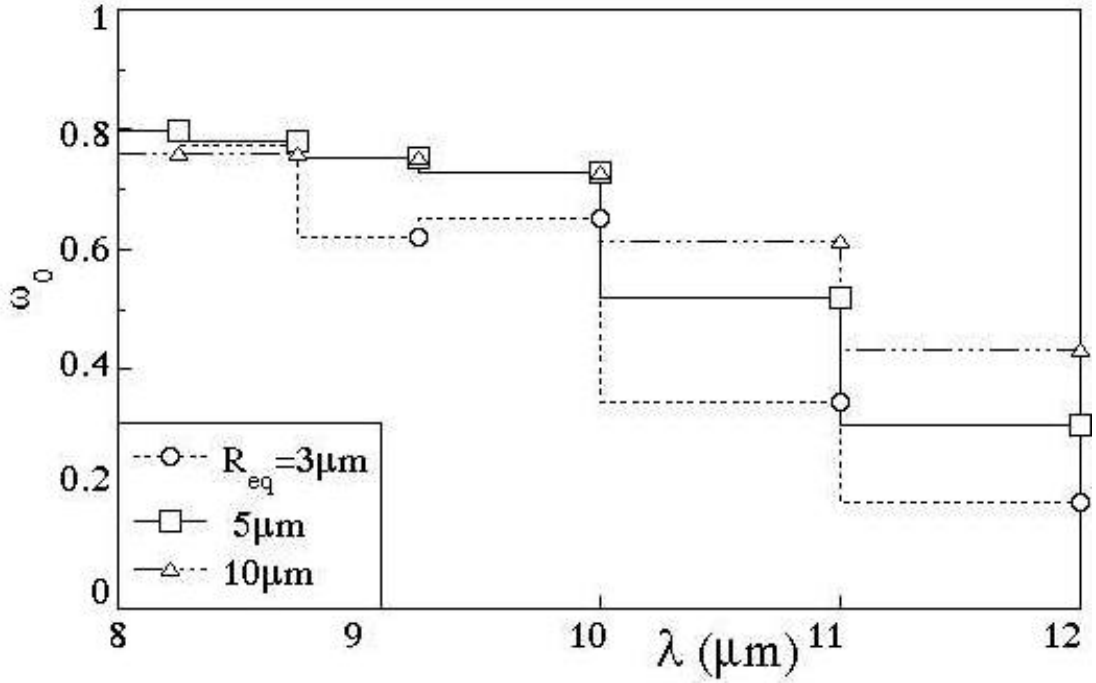

Figure 2b. Scattering albedo of water clouds.

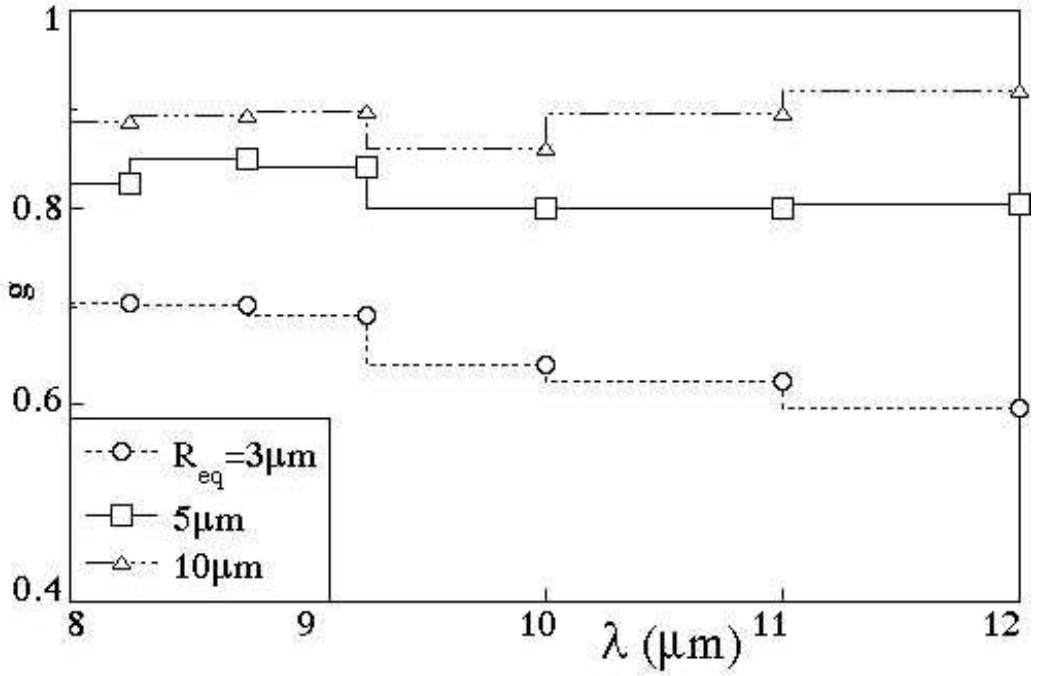

Figure 2c. Asymmetry parameter of water clouds.

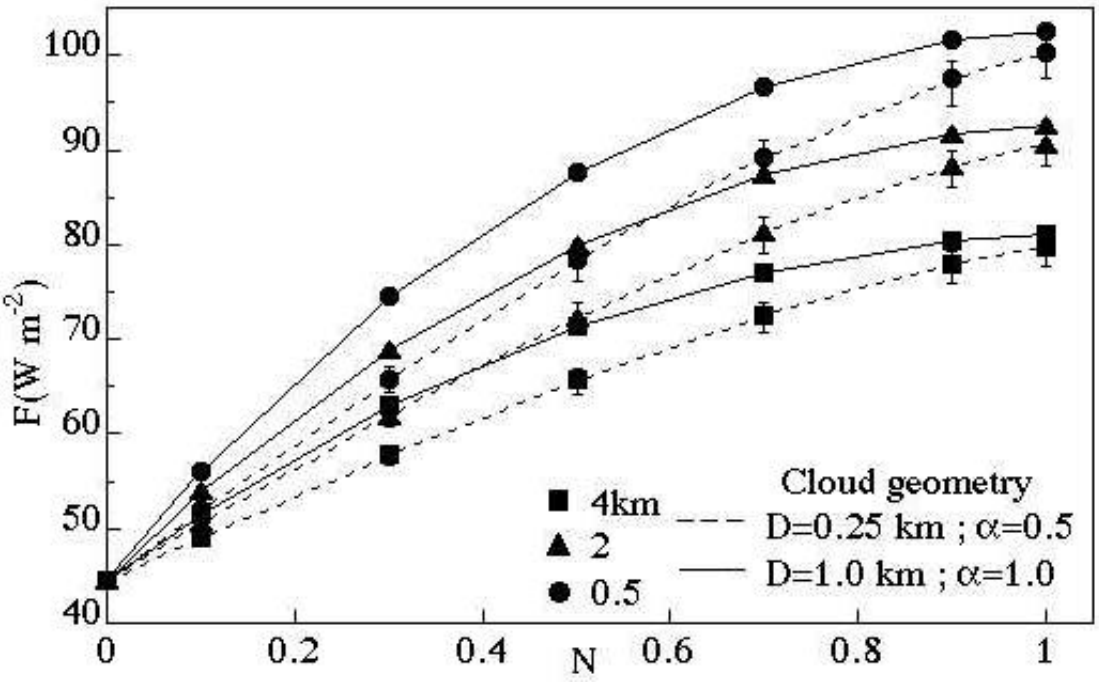

Figure 3a. MLS downward flux at surface.

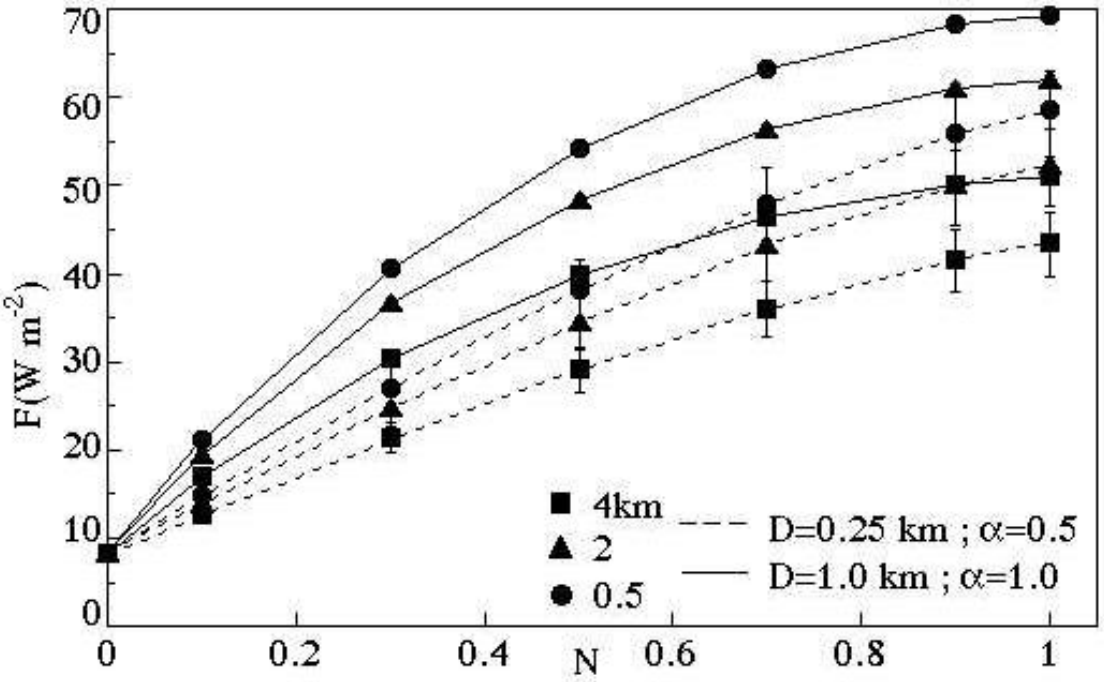

Figure 3b. MLW downward flux at surface.

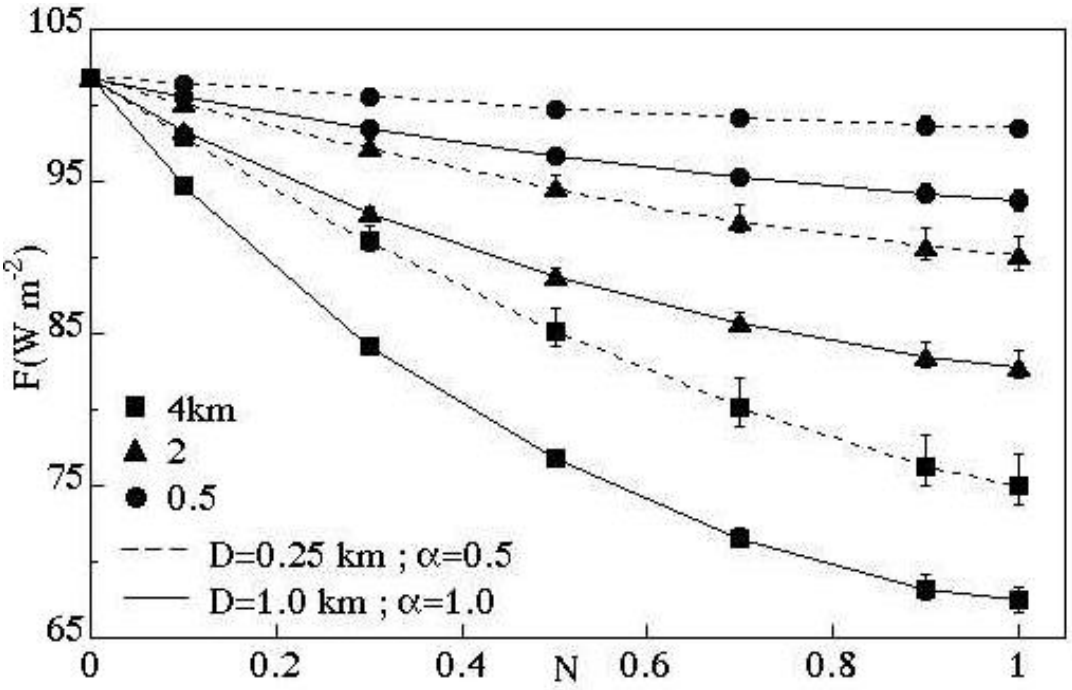

Figure 4a. MLS upward flux at 15 km.

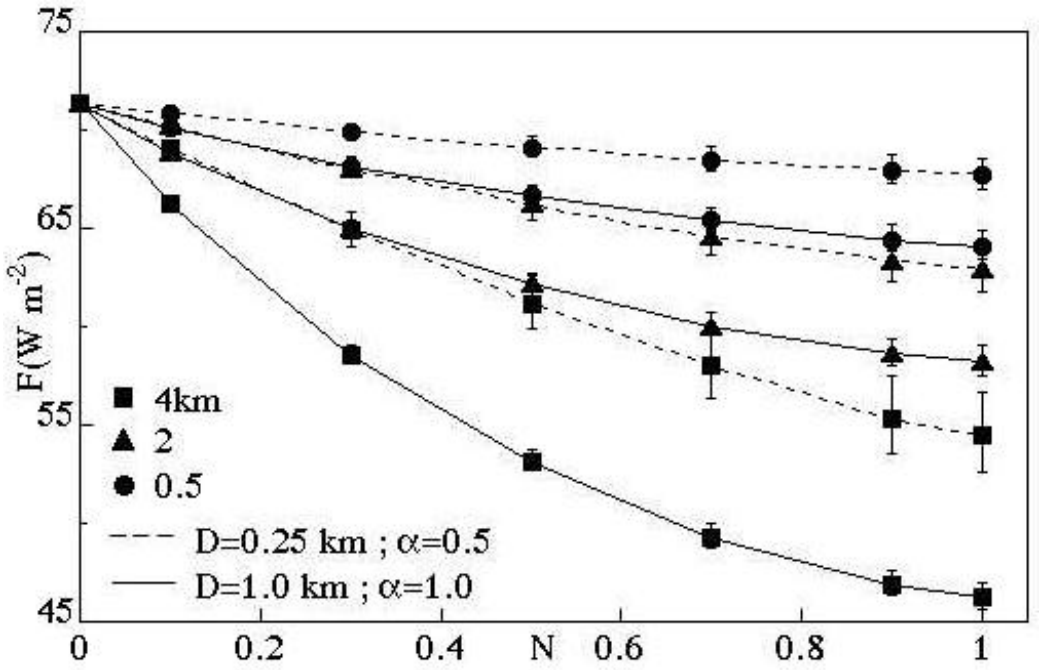

Figure 4b. MLW upward flux at 15 km.

given Z_b, the small cloud fluxes are greater than the large cloud fluxes because their tops are lower (warmer) than the tops of the large clouds. Again, the large cloud limit bars are smaller than the small cloud limit bars; the small cloud limit bars in Figure 4b are larger than those in Figure 4a.

The flux error for the no-scatter cloud approximation is

$$dF^{\uparrow\downarrow} = F^{\uparrow\downarrow}(\text{no-scatter}) - F^{\uparrow\downarrow} \tag{4}$$

The MLS and MLW errors for downward flux at the surface is shown in Figures 5a and 5b. There is no error for the clear-sky case; the lines were not extended to zero at N=0 in order to increase clarity. In both Figures 5a and 5b, the absolute value of the error is less than 1 $W*m^{-2}$ for large clouds. This is not surprising since the black cloud approximation also works for these optically thick clouds. The small cloud errors are larger, increasing in magnitude from around –0.5 $W*m^{-2}$ for N=0.1 to up to -3.5 $W*m^{-2}$ at N=1. This is considerably better than the black cloud approximation, which has a maximum MLW error of almost 18 $W*m^{-2}$. The no-scatter error is negative; it underestimates the surface flux. The no-scatter approximation cannot account for the increase in surface flux due to the scatter of surface emission from the cloud bottom back down to the surface; it has to underestimate the surface flux.

The errors for the upward flux at 15 km are shown in Figures 6a and 6b. Figures 6a and 6b are similar. The error increases almost linearly from around 0.5 $W*m^{-2}$ at N=0.1 to 4.5 $W*m^{-2}$ at N=1. This is roughly the same as the error for the black cloud approximation. Notice the error is positive in this case; the no-scatter overestimates the 15-km flux. The flux at 15 km is primarily due to emission by the cloud.

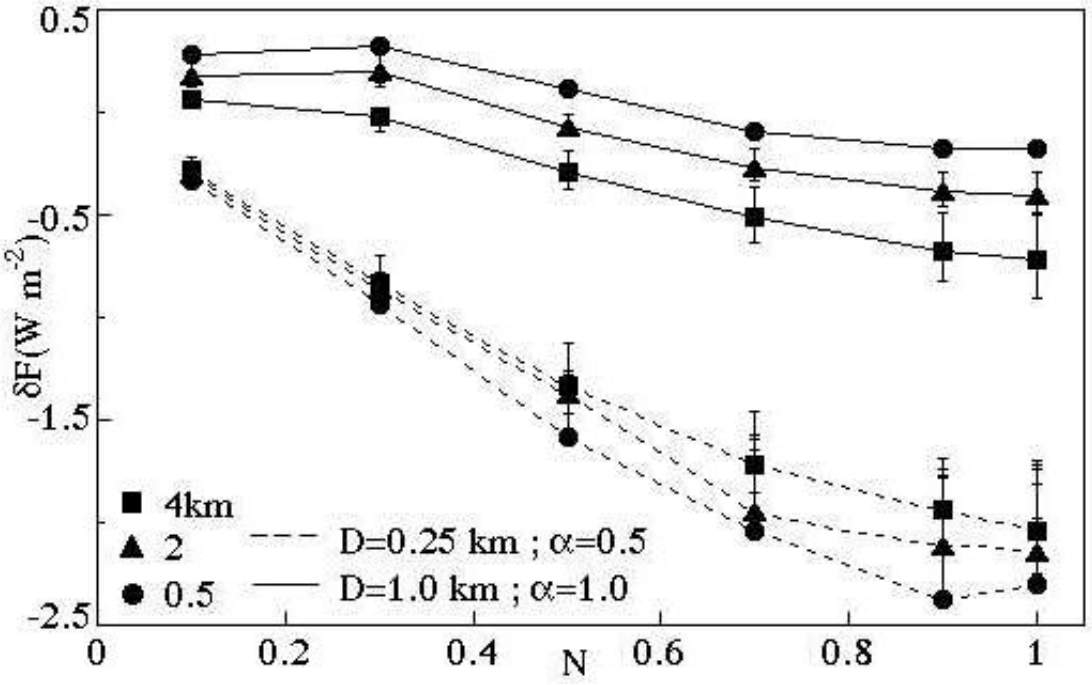

Figure 5a. MLS downward flux error at surface.

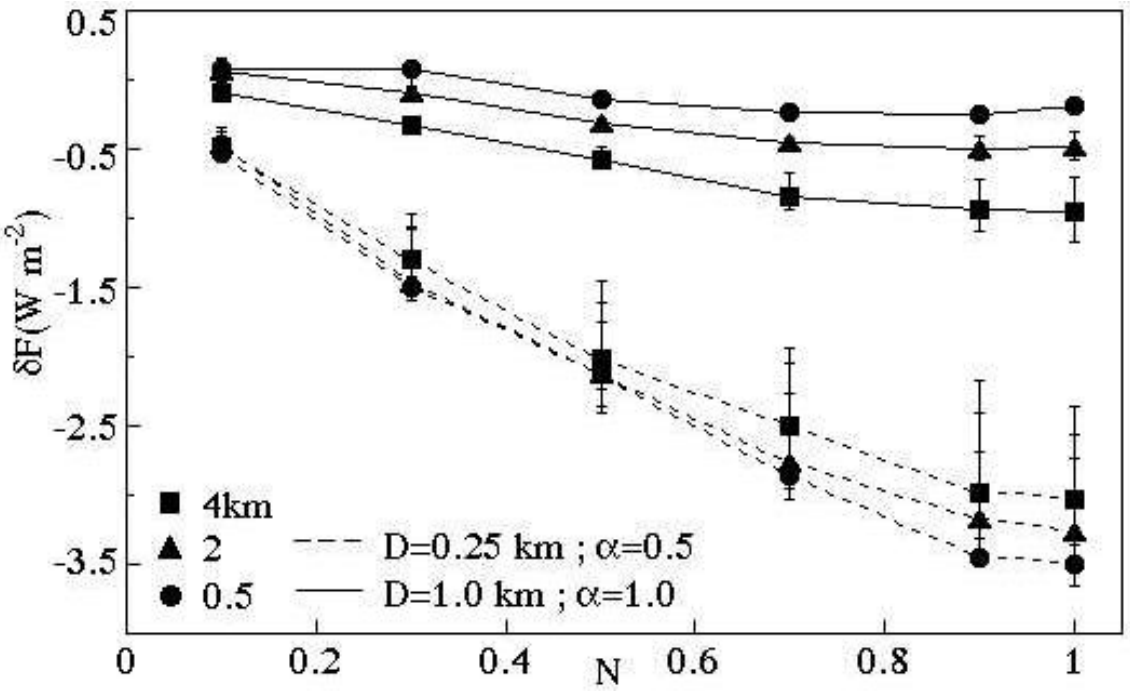

Figure 5b. MLW downward flux error at surface.

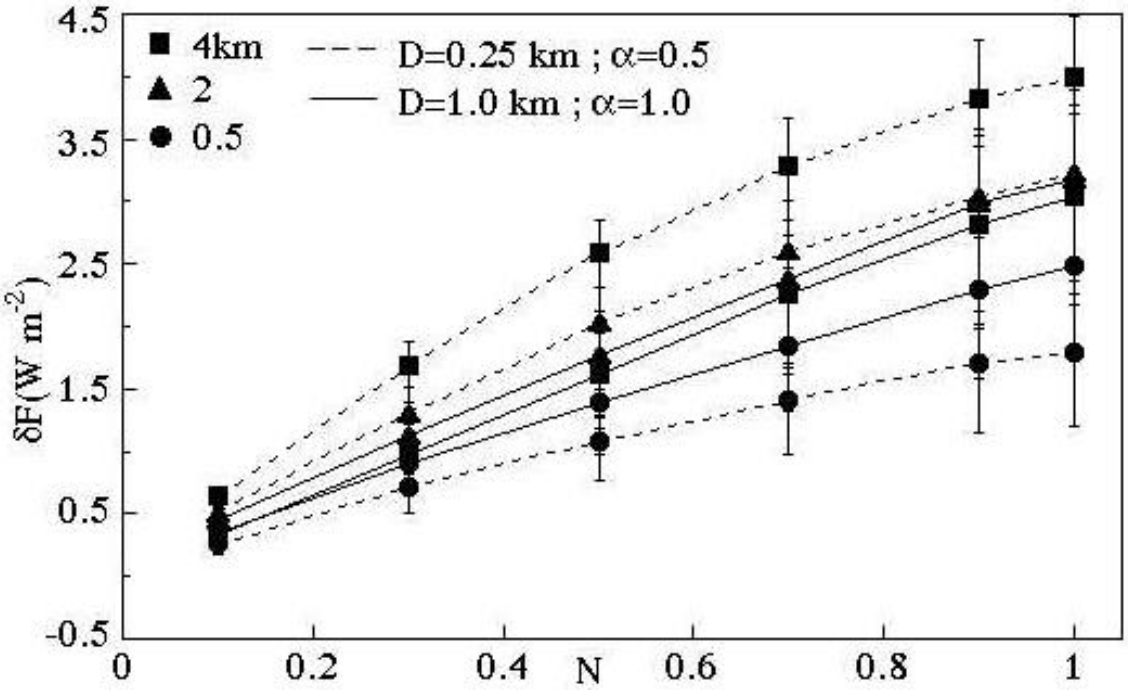

Figure 6a. MLS upward flux error at 15 km.

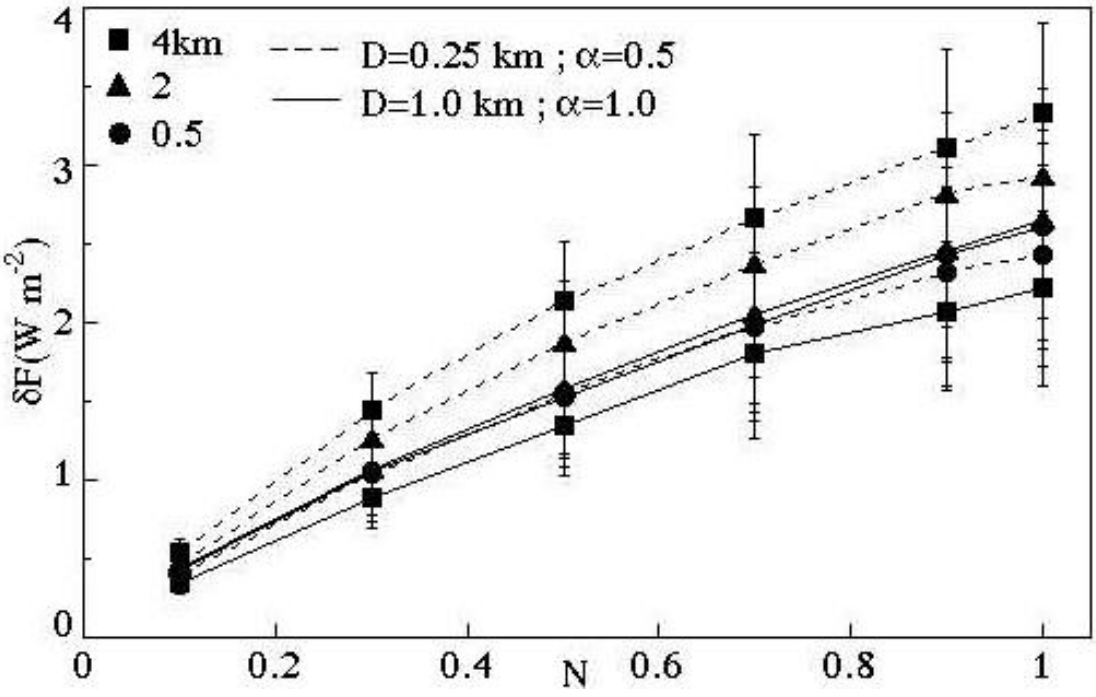

Figure 6b. MLW upward flux error at 15 km.

Scattering reduces emission from the clouds because it traps a cloud's emission within itself. The no-scatter approximation cannot account for this trapping effect; it has to overestimate the upward flux.

Conclusions

The no-scatter approximation worked quite well for surface fluxes, significantly improving on the black cloud approximation for optically thinner clouds. The no-scatter approximation was not significantly better than the black cloud approximation for upward fluxes above the clouds. Overall, it seems quite reasonable to use this approximation in future versions of MDTERP.

Acknowledgments

This paper was sponsored in part by the U.S. Department of Energy's Atmospheric Radiation Measurements (ARM) Program under grant DEFG0294ER61746.

References

Ellingson, R. G., and E. E. Takara, 1999: MDTERP—A narrowband longwave radiation model with a graphical user interface. This proceedings.

Ellingson, R. G., 1982: On the effects of cumulus dimensions on longwave irradiance and heating rates. *J. of Atmos. Sci*., **39**, 886-896.

Howell, J. R., and M. Perlmutter, 1964: Monte Carlo solution of thermal transfer through radiant media between gray walls. *J. Heat Transfer*, **86**, 116-122.

Hu, Y. X., and K. Stamnes, 1993: An accurate parameterization of the radiative properties of water clouds suitable for use in climate models. *J. of Climate*, **6**, 728-742.

McClatchey, R. A., R. W. Fenn, J.E.A. Selby, F. E. Volz, and J. S. Garing, 1971: Optical properties of the atmosphere (rev.). *Rep. AFCRL-71-0279*, 85 pp., Air Force Cambridge Res. Lab., Bedford, Massachusetts.

Takara, E. E., and R. G. Ellingson, 1999: Broken cloud field longwave scattering effects. *J. of Atmos. Sci*. Accepted.